Time Domain Model for Costas Loop Based QPSK Receiver

Maarten Tytgat, Michiel Steyaert and Patrick Reynaert
K.U. Leuven ESAT-MICAS
Kasteelpark Arenberg 10
B-3001 Leuven, Belgium
maarten.tytgat@esat.kuleuven.be

***Abstract*—A complete Matlab model is made for a millimeter wave wireless communication system including a four-phase Costas loop for carrier recovery and QPSK demodulation. Simulation results are presented to demonstrate the dynamic behaviour of the Costas loop and the effects of noise, linearity and bandwidth limitations. The time domain results are compared to the frequency domain transfer function derived from the Costas loop parameters.**

I. Introduction

The continuous demand for increasing data rates has pushed the operating frequency of wireless communication systems into the millimeter wave region. Larger bandwidths are thus available, allowing higher data rates with less complicated modulation schemes such as ASK, BPSK and QPSK.

An important issue when dealing with these high frequencies and high data rates is the problem of carrier recovery. Coherent detection requires a good phase and frequency reference with respect to the carrier of the RF signal.

If carrier recovery has to be done at baseband, high speed A/D-converters are needed, increasing power consumption and design complexity [1].

The carrier recovery can also be performed in the analog domain. Three important techniques are known: differential demodulation using a delay line to mix with a previous symbol, frequency multiplying and the Costas loop.

The problem with a delay line is that it has to provide a delay of one symbol period. For data rates in the order of several $\mathrm{Gbit/s}$, that would mean delay lines with lengths in the order of tens of millimeters. Furthermore, the data rate is fixed by the length of the delay element [2].

Using frequency multiplying would require circuits working at twice the carrier frequency for BPSK and four times the carrier frequency for QPSK, which is unrealistic for frequencies exceeding $100\mathrm{GHz}$.

The Costas loop is therefore a suitable candidate for carrier recovery and demodulation at millimeter wave frequencies, as already demonstrated in [1].

This paper presents a Matlab model and simulation results of a wireless communication system operating at $100\mathrm{GHz}$. Time domain simulations allow to analyze the dynamic properties and the behavior in the presence of noise of the Costas loop. The paper starts with the operation of the four-phase Costas loop and the discrete time equivalent. Then, simulation results are shown of the complete system with realistic quantities for data communication around $100\mathrm{GHz}$ with $\mathrm{Gbit/s}$ data rates.

II. The QPSK Costas loop

A. Operation

The Costas loop was first proposed by J. Costas as a phase tracker for (suppressed-carrier) AM signals [3]. It was later modified to demodulate QPSK and MPSK signals [4], [5]. The circuit diagram of the four-phase Costas loop is shown in Fig. 1a. Suppose the RF signal V_{RF} is QPSK modulated:

$$V_{RF} = I(t)\sin(\omega t + \theta) + Q(t)\cos(\omega t + \theta) \tag{1}$$

Where $I(t)$ and $Q(t)$ can be ± 1, varying at the symbol rate. Amplitudes are disregarded for simplicity. This signal is multiplied with an LO with the same frequency and an instantaneous phase of θ' and a 90° phase shifted version of this LO. Then after low pass filtering the signals are:

$$Z_I(t) = I(t)\cos\phi - Q(t)\sin\phi \tag{2}$$
$$Z_Q(t) = I(t)\sin\phi + Q(t)\cos\phi \tag{3}$$

With $\phi = \theta - \theta'$. If we assume that the pahse error is always $|\phi| < 45^\circ$, the output of the limiters is:

$$L_I(t) = I(t) \tag{4}$$
$$L_Q(t) = Q(t) \tag{5}$$

The error signal is then:

$$\begin{aligned}\epsilon(t) &= Z_Q L_I - Z_I L_Q \\ &= I^2(t)\sin\phi + Q(t)I(t)\cos\phi \\ &\quad - I(t)Q(t)\cos\phi + Q^2(t)\sin\phi \\ &= 2\sin\phi \\ &\approx 2\phi \qquad \text{(for very small } \phi\text{)}\end{aligned} \tag{6}$$

This way, a phase error signal is obtained, which can adjust the VCO in order to maintain phase and frequency lock. If the absolute phase error is initially larger than 45°, the loop will still lock, but the received constellation will have a fixed rotation of a multiple of 90° with respect to the transmitted constellation.

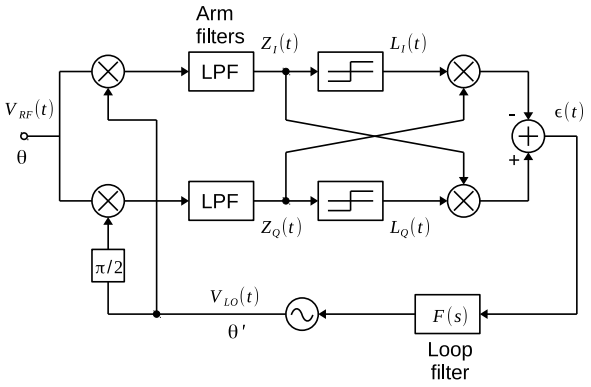

(a)

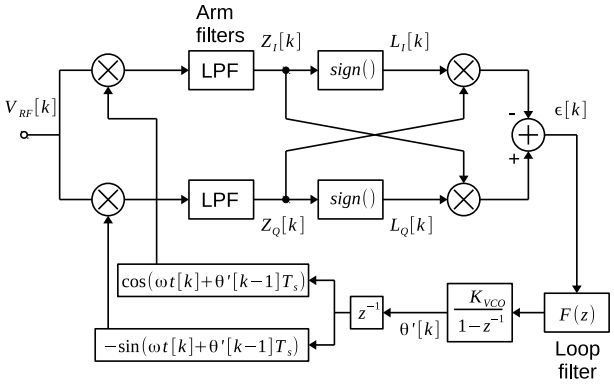

(b)

Fig. 1. Schematic of the four-phase Costas loop (a) and discrete time equivalent (b).

B. Discrete time implementation

In order to make a model of the Costas loop in Matlab, the continuous time circuit has to be transformed to the discrete time domain. This is shown in Fig. 1b. In this schematic, the variable $t[k]$ is the sampled time and T_s is the sampling period. The VCO is represented by integrating the output of the loop filter and multiplying by K_{VCO} to get the instantaneous phase θ' for the $\sin$ and $\cos$ functions.
This discrete-time model can be directly translated into Matlab code. The filters are implemented as IIR filters using difference equations.

III. Simulation of communication link

A. System overview

In order to reflect a realistic situation, the complete transmitter-receiver system of Fig. 2 was translated into Matlab code and simulated in the time domain. The transmitter can be configured for a certain carrier frequency f_c, symbol rate R and output power P_{Tx}. Additionally, certain non-idealities can be added, such as phase and frequency steps and frequency drift.

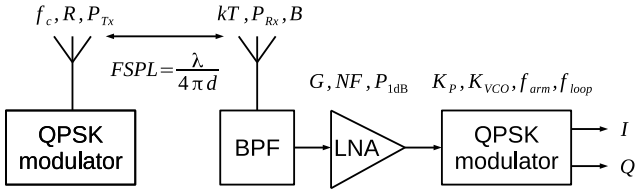

Fig. 2. Overview of the simulated wireless data communication link.

TABLE I
Costas loop design parameters

Carrier frequency	f_c	100GHz
Symbol rate	R	4GBd/s
Data rate	D	8Gbit/s
Phase constant	K_P	0.75V/rad
VCO gain	K_{VCO}	5GHz
Arm filter pole	f_{arm}	8GHz
Loop filter pole	f_{loop}	200MHz
RF bandwidth	B	10GHz
Distance	d	10cm
Free space path loss	FSPL	52.4dB
Transmitted power	P_{Tx}	0dBm
Received power	P_{Rx}	−52.4dBm
Noise Figure LNA	NF_{LNA}	10dB
SNR at output LNA	SNR_{LNA}	11.5dB

The channel is modelled with frequency and distant dependent free space path loss. The antenna gains are assumed to be zero. White noise is added at the receiver antenna as a gaussian distributed random number with $\sigma = \sqrt{kT\frac{F_s}{2}}$ (F_s is the sampling frequency). The total noise power is determined by the input bandwidth B.
The receiver features an LNA with a gain G, noise figure NF and linearity specified by P_{1dB}.
The design parameters of the Costas loop are the coefficients of the arm filters and loop filter and the gains of the different blocks. In the following simulations, the arm and loop filters are implemented as first order low pass filters. The system thus resembles a second-order PLL, with a loop gain of $K_P K_{VCO}$. By definition, $K_P = \frac{\epsilon}{\phi}$ is the phase constant of the Costas loop and it is dependent on the gains within the Costas loop and the amplitude of the received signal.
The used parameters in the reported simulations are shown in table I. These numbers are realistic values for a transmitter and receiver in a modern CMOS technology at a carrier frequency around 100GHz.

B. Simulation results

To illustrate the phase detection mechanism of the four-phase Costas loop, an open loop simulation is performed by setting $K_{VCO} = 0$. The relevant signals are plotted in Fig. 3. Noise has not been included in this simulation.
The carrier is given a phase difference of 22.5° ($\pi/8$) with respect to the VCO. From the bottom right graph, the phase

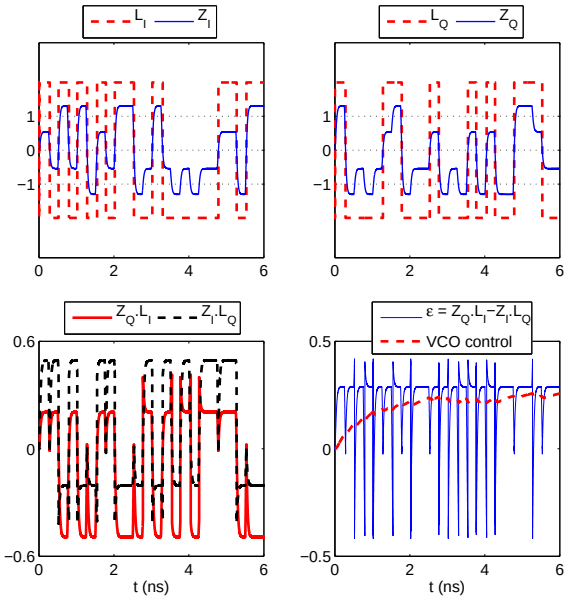

Fig. 3. Signals in the Costas loop for a phase difference of $\frac{\pi}{8}$ between carrier and VCO. The loop is cut in order to observe the phase dection mechanism.

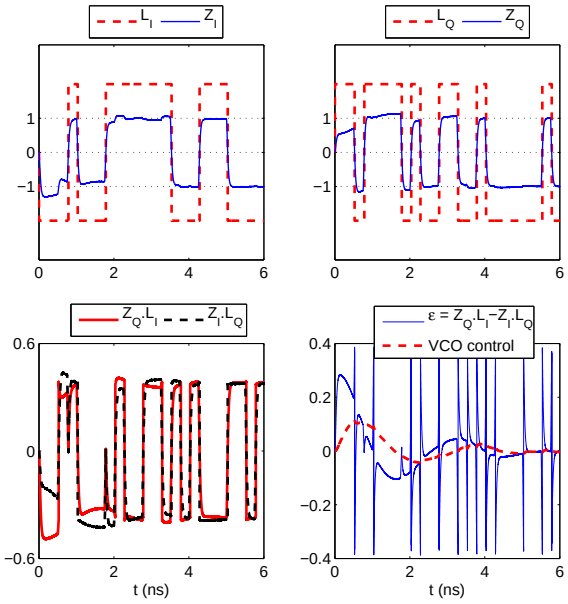

Fig. 4. Signals in the Costas loop for an initial phase difference of $\frac{\pi}{8}$, this time with the loop closed. The VCO frequency is adjusted so that the phase error is eliminated.

detector constant can be derived: $K_P = \frac{0.3V}{\pi/8} \approx 0.75V/rad$. The loop filter eliminates the spikes on the ϵ signal.

When the loop is closed ($K_{VCO} = 5\text{GHz/V}$), the phase tracking can be observed (Fig. 4).

The response of the loop to a frequency step of 100MHz is shown in Fig. 5. It shows the carrier frequency and the instantaneous VCO frequency. The maximum frequency step that can be allowed is determined by the loop dynamics in the same way as in a second order PLL [6].

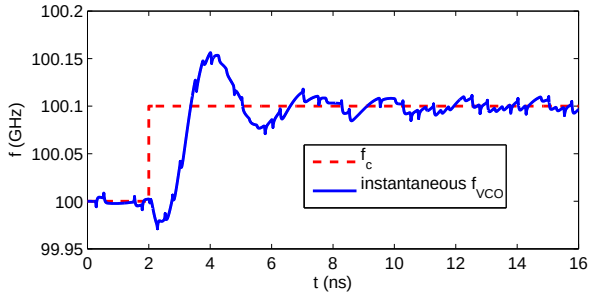

Fig. 5. Response to a frequency step of 100MHz.

To compare the time domain simulation results to the frequency domain predictions, simulations are performed with analog phase modulation on top of the QPSK modulation. The θ from formula 1 is varied at the modulation frequency f_m, with an amplitude $|\theta|$. The Costas loop will suppress force the VCO to have the same phase modulation, thus making $|\phi|$ zero. This will only succeed for low modulation frequencies. With increasing modulation frequency, the magnitude of the phase error $|\phi|$ is compared to the phase error transfer $E(s)$ function which is derived from the parameters of the Costas loop:

$$E(s) \equiv \frac{\phi(s)}{\theta(s)} = 1 - H(s) = \frac{s}{s + K_{VCO}K_P F(s)} \qquad (7)$$

As can be seen in Fig. 6, the time domain results show good agreement to the frequency domain predictions.

With the inclusion of noise, the received constellation looks like Fig. 7. This is a plot of the signals Z_I and Z_Q, i.e. before the limiters, sampled at the data rate. This result is obtained for a received signal strength of -52.4dBm and SNR of 21.5dB. Behind the LNA with a noise figure of 10dB, which is a realistic number in CMOS at 100GHz, the SNR is 11.5dB.

The corresponding eye diagram of the Z_I signal is plotted in Fig. 8.

The bit error rate can be simulated in function of the SNR at the output of the LNA. This is shown in Fig. 9. The noise at the input is increased, while the signal level is held constant so as not to change the K_P of the loop. For larger SNRs than 3.5dB, the simulation time needed to encounter a sufficient amount bit errors becomes too long. The typical waterfall curve is clearly observed.

IV. Conclusion

A complete time domain Matlab model has been presented for a wireless communication system at millimeter wave frequencies, using a four-phase Costas loop as carrier recovery circuit and QPSK demodulator.

The operation of the phase tracking mechanism has been illustrated and the equivalence to a second-order PLL has been shown with simulations.

By using realistic numbers, an idea is given about the quantities involved in high data rate wireless communication around

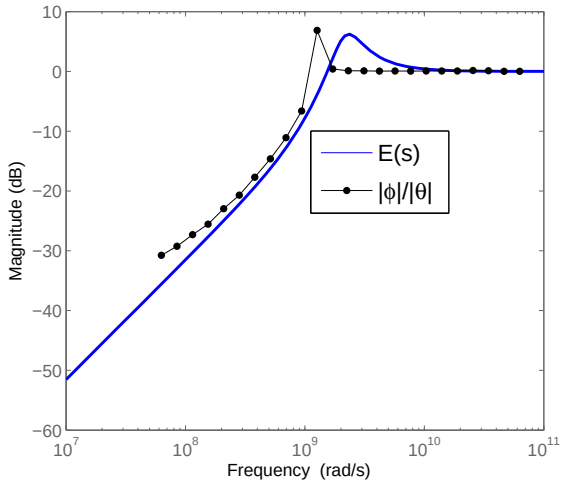

Fig. 6. Error transfer function $E(s)$ and time domain simulations of phase error.

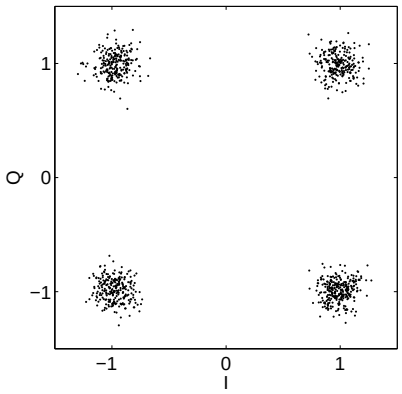

Fig. 7. Constellation plot for SNR $= 11.5$dB at output of LNA. The data rate is 8Gbit$/$s.

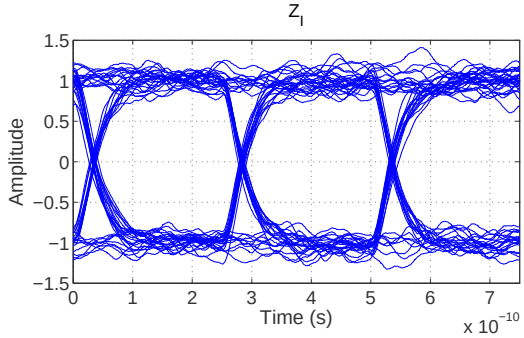

Fig. 8. Eye diagram of the Z_I signal. The data rate is 8Gbit$/$s.

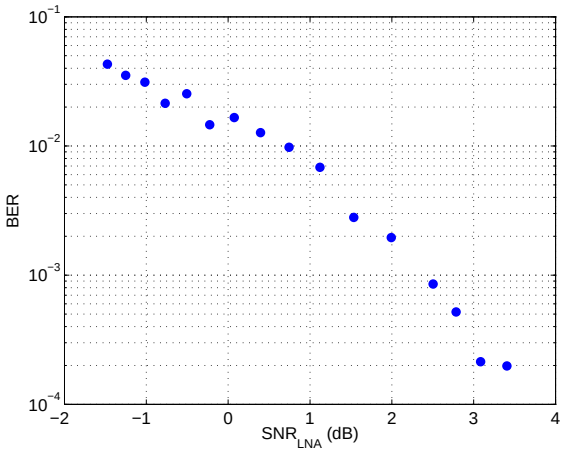

Fig. 9. Simulated Bit Error Rates in function of SNR at the LNA output.

100GHz.

The influence of noise is shown in the form of a constellation diagram, an eye diagram and a BER versus SNR graph. This model can be used to predict and optimize the performance of a Costas loop based receiver.

ACKNOWLEDGMENT

This research is partly supported by the ERC Advanced Grant 227680 (DARWIN).

REFERENCES

[1] S.-J. Huang, Y.-C. Yeh, H. Wang, P.-N. Chen, and J. Lee, "An 87GHz QPSK transceiver with costas-loop carrier recovery in 65nm CMOS," in *Solid-State Circuits Conference Digest of Technical Papers (ISSCC), 2011 IEEE International*, feb. 2011, pp. 168 –170.

[2] H. Takahashi, T. Kosugi, A. Hirata, K. Murata, and N. Kukutsu, "10-Gbit/s quadrature phase-shift-keying modulator and demodulator for 120-GHz-band wireless links," *Microwave Theory and Techniques, IEEE Transactions on*, vol. 58, no. 12, pp. 4072 –4078, dec. 2010.

[3] J. Costas, "Synchronous communications," *Proceedings of the IRE*, vol. 44, no. 12, pp. 1713 –1718, dec. 1956.

[4] C. Weber and W. Alem, "Demod-remod coherent tracking receiver for QPSK and SQPSK," *Communications, IEEE Transactions on*, vol. 28, no. 12, pp. 1945 – 1954, dec 1980.

[5] H. Osborne, "A generalized "polarity-type" costas loop for tracking MPSK signals," *Communications, IEEE Transactions on*, vol. 30, no. 10, pp. 2289 – 2296, oct 1982.

[6] F. M. Gardner, *Phaselock techniques*. John Wiley and Sons, July 2005.